university of groningen

kvi - center for advanced radiation technology

Super-Heavy Dark Matter as a source of Ultra-High Energy Cosmic Rays

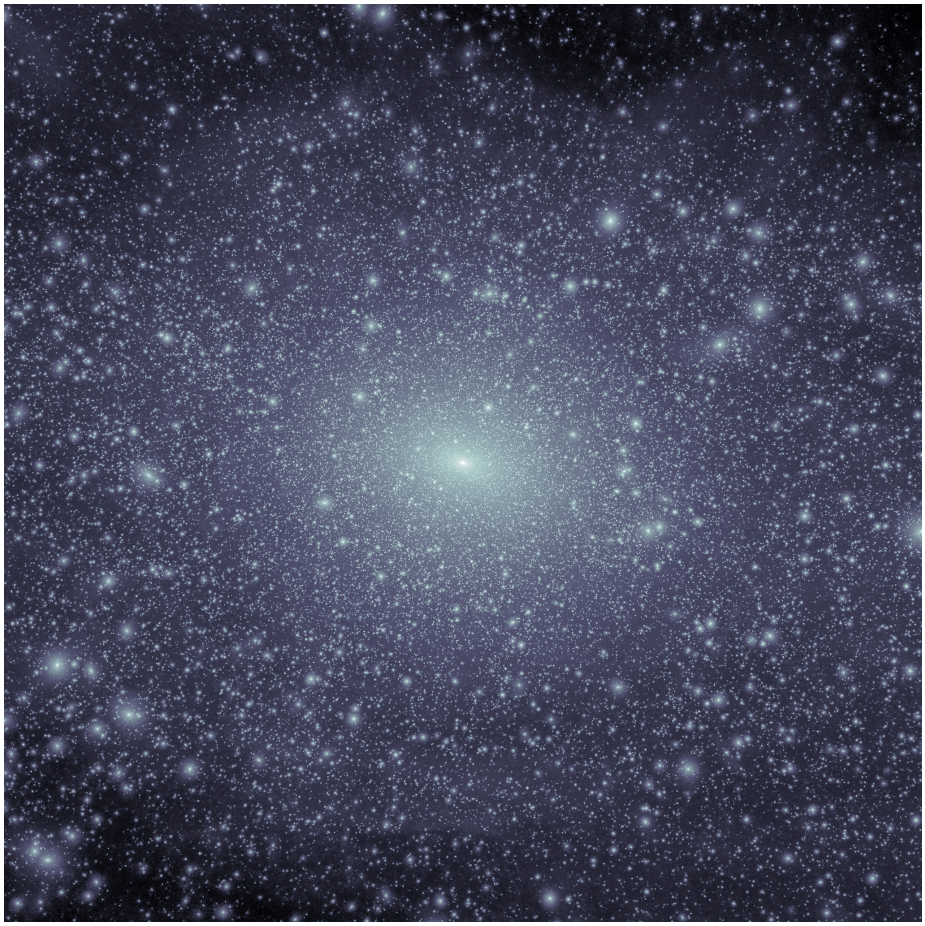

Author:
Sybrand Zeinstra

Supervisor:
Dr. Olaf Scholten

This page is intentionally (almost) left blank.

university of groningen

kvi - center for advanced radiation technology

Super-Heavy Dark Matter as a source of Ultra-High Energy Cosmic Rays

Author:
Sybrand Zeinstra

Supervisor:
Dr. Olaf Scholten

12th July 2016

Abstract

We have studied superheavy dark matter as a possible source of ultra-high energy cosmic rays. Following the non-thermal instant preheating mechanism, superheavy dark matter can be created in the early universe, directly after inflation. The mass of these particles can range from 10^{14} to 10^{18} GeV. This mass is large enough to create cosmic rays with an energy above the GZK cut-off upon annihilation of two dark matter particles. Annihilation of dark matter is more prevalent near the core of the galactic dark halo, and in smaller, dense clumps called subhalos. An estimate of the annihilation cross section yielded a rather high upper limit on the order of $\sigma \sim 10^{-8}$ cm^2. Around the GZK cut-off there might not be a clear correlation between the arrival direction of extra-galactic ultra-high energy cosmic rays, and the local matter distribution. This correlation could become significant for energies above 10^{20} eV. Observation of anisotropy on the galactic scale could also support this top-down model, but no anisotropy has been observed so far.

Acknowledgements

One does not simply write a bachelor thesis alone. Over the last few months working on this thesis I often got stuck, and needed to take a fresh look at the problems I was tackling. In this regard, I would first and foremost thank my supervisor, Olaf Scholten, for his valuable advice. Instead of focusing on calculations, he made me think about and understand the physics of the problem. The calculations and formulae then come more easily. I really liked it that he is always open for a discussion or good conversation, not only about the matter in this thesis, but also about things like education at this university. I also would like to thank him for giving us the opportunity to present a poster about our thesis at the ARENA conference.

For the poster Rick and I had to prepare for the conference, Qader Dorosti has been of great help. He provided us with a poster of his that we could use as template and showed us the tools to work on the poster. Furthermore, he took the time to give us good feedback, which resulted in a clear and interesting poster.

Finally, I want to thank the other students in the astroparticle physics group for the good atmosphere, and sometimes the nice chats we had in our "studententuin". In these weeks at the kvi, I had many lunches with Bas, giving us some time to talk about our daily activities and other interesting things. It is good to take a break sometimes, and if the weather allowed it, we would go outside to enjoy the sunshine next to the moat of the kvi. Bas also kept me company on our daily cycle trip along the water of the Reitdiep to the kvi and back which, especially when facing a headwind, seems longer than it actually is. Luckily we could drop by Anno in the Nijenborgh for a nice cookie on our way back.

Contents

Chapter 1

Introduction

Cosmic rays are energetic particles of extraterrestrial origin that have been detected as early as 1911 when Victor Hess measured the amount of radiation at an altitude of several kilometers up in the atmosphere. He concluded that this radiation had an extraterrestrial origin. Today, the energy spectrum of the detected cosmic rays is relatively well known, except for the part with energies above ~ 1 EeV, also known as the *ankle*. At these very high energies, the spectrum eventually falls off due to accelerators of particles not being powerful enough, or due to the Greisen-Zatsepin-Kuzmin (GZK) effect. This effect originates from interactions of high-energetic particles with an energy of $\sim 4 \times 10^{19}$ eV or larger with the Cosmic Microwave Background (CMB) photons [1, 2].

Different models have been created in order to provide an explanation for cosmic rays with these ultra-high energies. The models can be divided into two classes. Bottom-up models are models in which the cosmic rays are accelerated. This can for example be acceleration of particles in shock waves, or more violently near black holes or in supernovae. Top-down models are models where cosmic rays are created in the decay or annihilation of particles or topological defects.

This thesis aims to look into Super-Heavy Dark Matter (SHDM), consisting of particles with a mass in the range of $\gtrsim 10^{13}$ GeV as a possible origin of cosmic rays, and of special interest are ultra-high energy cosmic rays (UHECRs). If UHECRs are created in the decay or annihilation of SHDM particles, it would form a link between two different areas of physics.

1.1 Dark Matter

One of the first arguments one always hears for the existence of dark matter comes from the observation of rotation curves for galaxies. More recent measurements by the Planck satellite estimate that only $\sim 5\%$ of the total energy budget in the universe is spent on visible, luminous matter. The largest remaining part is mostly dark energy ($\sim 68\%$) which causes expansion of the universe, and the rest ($\sim 27\%$) dark matter [3]. In chapter 2 we will give an overview of different theories about what makes up dark matter.

1.2 Cosmic ray spectrum

The number of cosmic rays that arrive at Earth strongly depends on the energy. The spectrum follows a power law, with the differential flux being given by [4]:

$$\frac{dF}{dE} \propto E^{\gamma}\,, \tag{1.1}$$

where γ lies between -2.7 and -3.1 depending on the part of the spectrum. The cosmic ray energy spectrum is shown in figure 1.1. Figure 1.2 on page 3 shows the scaled spectrum, distinguishing features at the highest energies. In this figure also the maximum energies of the Tevatron and LHC are indicated. We see that part of the cosmic ray spectrum has energies larger than we are able to reach in particle accelerators. Therefore studying cosmic rays means using the biggest accelerator we can find: the Universe. In this spectrum we can distinguish different regimes. In the region up to energies of 5×10^{15} eV, charged cosmic rays can be contained in the magnetic field of galaxies, including our own. For higher energies the spectrum steepens. The point where this happens is called the knee. Above 5×10^{18} eV the spectrum gets slightly flatter, before it is strongly suppressed for energies above 5×10^{19} eV [5].

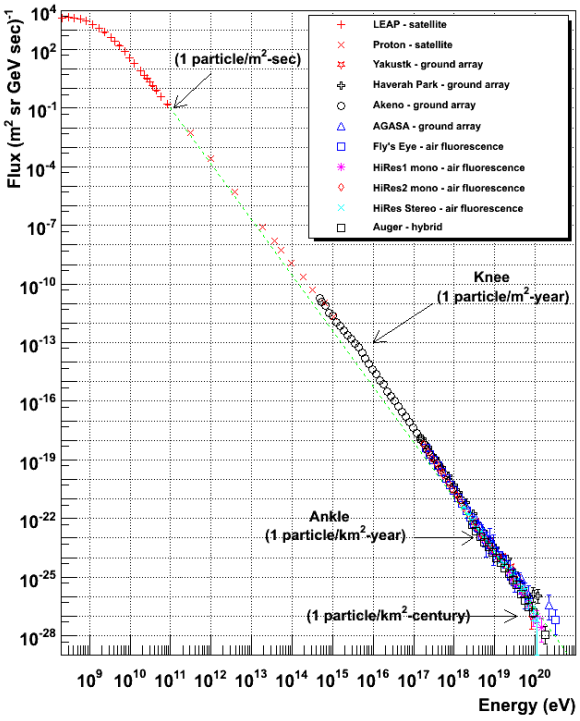

Figure 1.1: The cosmic ray spectrum obtained from various experiments plotted together. The data points follow a power law. Source: [6]

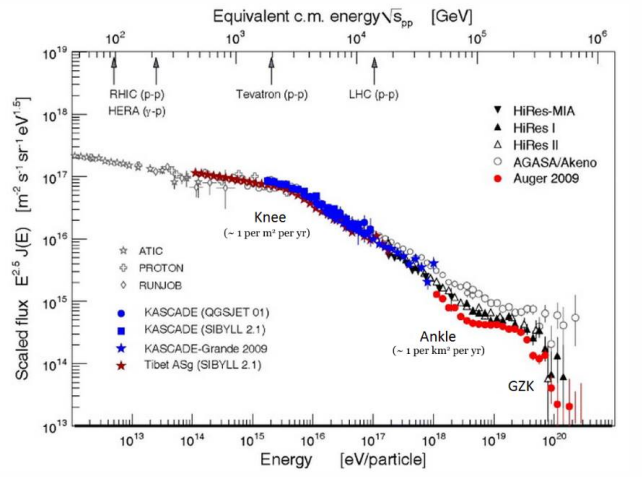

Figure 1.2: Highest-energy part of the cosmic ray spectrum, scaled with a factor $E^{2.5}$. Source: [7]

1.2.1 GZK cut-off

The Greisen-Zatsepin-Kuzmin cut-off is a process that limits the flux of the cosmic rays with energies of $\sim 4 \times 10^{19}$ eV, that was proposed in 1966 [1, 2]. Figure 1.2 shows spectrum of the highest-energy cosmic rays, scaled with a factor $E^{2.5}$. The GZK cut-off is indicated in this figure. Ultra-high energy protons can interact with CMB photons and create pions via the following processes

$$p + \gamma_{\text{CMB}} \rightarrow p + \pi^0 \text{ or } n + \pi^+ \,. \tag{1.2}$$

In this process, the proton loses about 20% of its energy. As protons with energies above this GZK cut-off travel through space, they lose energy and will thus end up at energies lower than the cut-off energy. Using the values presented in [2] for a CMB photon density of $n_\gamma \approx 550$ cm^{-3} and a cross section for this reaction of $\sigma = 1 \times 10^{-28}$ cm^2, cosmic rays with energy larger than the GZK cut-off have a mean free path of

$$\lambda = \frac{1}{n_\gamma \sigma} \approx 6 \text{ Mpc}. \tag{1.3}$$

This means that if we observe cosmic rays with energies above the GZK cut-off, they must come from within a distance of around 50 Mpc. High-energy cosmic rays above the knee are largely protons, but data from the Pierre Auger observatory places limits on the photon fraction that range from 2.0% at 10^{19} eV, to 31% at the cut-off energy of 4×10^{19} eV [8].

1.3 Overview thesis

In this thesis we will aim to connect the annihilation of SHDM to to the origin of cosmic rays. As means of introduction, we will present in chapter 2 an overview of the various theories on the kind of matter that makes up the dark matter content. In the following chapter we will briefly discuss the era of inflation, to give some background information, and to familiarise the reader with concepts that will return later in this thesis. In chapter 4 we will discuss a few creation mechanisms for creating dark matter, where we have focused on the instant preheating mechanism. It is of interest to determine the relative amount with which this mechanism can produce particles, as the current abundance of dark matter in the universe is known. This we will address in chapter 5. In chapter 5 we will also discuss, in case of decaying dark matter, the lifetime, and a possible annihilation mechanism of dark matter. Subsequently we shift our focus, and in chapter 6 we look at the distribution of dark matter in the part of the universe closest to us: the halo of our own galaxy. We will use the information from previous chapters in chapter 7 to make an estimate of the cross section of dark matter annihilations required to be consistent with the observed cosmic ray flux.

Chapter 2

Dark Matter models

As to what makes up this unseen matter in the universe, different theories have been developed. Here we will discuss different dark matter particle candidates that have been proposed. We can distinguish two main classes of dark matter candidates, baryonic and non-baryonic. Baryonic dark matter would be clustered in MACHOs, massive astrophysical compact halo objects. Non-baryonic matter could consist of WIPMs, weakly interacting massive particles. In this chapter, we will briefly discuss some of the proposed dark matter candidates.

2.1 MACHOs

MACHOs consist of astrophysical objects that are too faint to be detected. The number density of stars with a certain mass m that are formed follows

$$\frac{dn}{d\ln m} \propto m^{-x}\,, \tag{2.1}$$

with $x = 2.35$, as was established by Salpeter in 1955 [9]. However this relation is assumed to hold in a certain range. This means that the higher mass objects, as well as lower mass objects are not taken into account. The lower mass is usually set at $0.08 \pm 0.01 M_{\odot}$ [10]. In objects with masses lower than this limit, no nuclear fusion can take place and any produced radiation is due to gravitational effects. These objects are called brown dwarfs, which are hard to detect because of their low luminosities. The method astrophysicists have used in observations was based on microlensing. In short, this means that the brightness of a background star changes when an object moves in front of the star. This explanation is however disfavoured because of lack of observations of brown dwarfs [11].

2.2 WIMPs

WIMPs, weakly interacting massive particles, are relic particles that are formed in the early universe. These WIMPs are non-baryonic, meaning the particles we are looking for are either massive neutrinos or some more exotic particles. This

could for example be particles from a supersymmetric extension of the Standard Model. Since MACHOs are disfavoured, dark matter likely consists of WIMPs.

2.2.1 Sterile neutrinos

According to the standard model, neutrinos are massless. From the observation of neutrino oscillations it was established that neutrinos do have mass. Within the Standard Model, normal neutrinos have left-handed chirality, but there may exist right-handed neutrinos too. The standard, left-handed neutrinos only interact via the weak interaction, and interact very little with ordinary matter. Right-handed neutrinos do not interact via the weak interaction either, this gives them the name "sterile neutrinos". The only way in which these sterile neutrinos interact is via flavour mixing with left-handed neutrinos [12]. In the early universe, only left-handed neutrinos are formed, since only they interact with other matter. These left-handed neutrinos then slowly mix into right-handed neutrinos. This is mechanism has also been called a freeze-in mechanism. Sterile neutrinos can be a plausible candidate to make up the dark matter content of the universe, since they have no interaction with ordinary matter, except with their left-handed counterparts, and this makes them likely to survive long enough to be present today. The mass of these particles is suggested to lie on the order of ~ 10 keV, in order to be a candidate for dark matter [12, 13]. Observations of emission lines around $E = (3.55 - 3.57) \pm 0.03$ keV [14] and 3.52 ± 0.02 keV [15] are consistent with the decay of a 7.1 keV sterile neutrino.

2.2.2 Axions

Axions are particles that were first proposed as a solution to the CP-problem in QCD. The QCD Lagrangian looks as if it is symmetrical under CP, charge and parity, transformations, also within experimental limits. A sign of strong CP-violation would be the observation of the neutron electric dipole moment, which has not been detected. There is within the theory no reason not to have symmetry breaking interactions, but from experiments, these effects must be very small. In fact, the parameter corresponding to symmetry breaking effect must be so small, that it leaves us with a fine-tuning problem, as there is no explanation for such a small value. This can be solved by introducing a new symmetry, which predicts a new, pseudoscalar particle. Thus the axion was proposed as a particle that could break the CP symmetry. If the axion is light enough (but above 1 μeV) it could account for part of the dark matter in the universe. For an axion mass of $\approx 20\mu$eV, axions could account for the entire dark matter content [16].

2.2.3 Supersymmetric particle

Another proposed dark matter candidate is a supersymmetric particle. These particles could be formed in the reheating phase after inflation. For the highest possible reheating temperature $T_r = 10^9$ GeV, the minimum masses of these particles must be above 3×10^{11} GeV. If dark matter consists of the lightest supersymmetric particle, its mass must be at least two orders of magnitude above the minimum, in order to explain ultra-high energy cosmic rays [17].

Chapter 3

Inflation

The early universe underwent a phase of rapid vacuum driven expansion called inflation. Inflation solves many problems in modern cosmology [10]. First of all, it solves the flatness problem. Our current universe seems remarkably flat, with data from the Planck satellite placing the deviation from a flat universe (where $\Omega = 1$) at $|\Omega - 1| = 0.000 \pm 0.005$ [3]. From inflationary models, the universe should have expanded with ~ 60 e-foldings to explain the flatness of the current universe. It also helps explain why the CMB looks (almost) isotropic, while regions of the sky separated by more than 1° are seemingly too far away to have had causal contact. If one includes inflation, these regions could have been in causal contact before inflation took place. It also explains why we do not see any magnetic monopoles in our universe, since the density of monopoles formed in the very early universe should have been decreased rapidly during inflation. Altogether, inflation is a well established theory in cosmological physics.

In this chapter we give a short description of the inflationary period in the early universe and the start of the reheating phase following inflation, and we introduce some concepts that will return in later chapters.

3.1 Friedmann Equations

Assuming that the universe is homogenous and isotropic, the metric of spacetime is the Friedmann-Lemaître-Robertson-Walker (FLRW) metric, given by

$$c^2 d\tau^2 = c^2 dt^2 - R^2(t) \left(\frac{dr^2}{1 - kr^2} + r^2 d\psi^2 \right) . \tag{3.1}$$

Where the interesting parts are $R(t)$, which is the scale factor of the universe, and k, which is a curvature term that is connected to the geometry of the universe. $k = +1$ corresponds to a closed universe, where an adventurer setting off in a single direction will eventually come back to the same point, like walking on the surface of a sphere. $k = -1$ corresponds to an open universe, where our adventurer can travel infinitely far without ever returning to his starting point. This universe is shaped like a saddle. Finally, $k = 0$ corresponds to an infinite but flat universe. Friedmann described the evolution of the radius $R(t)$ in the

eponymous Friedmann equation

$$\dot{R}^2 - \frac{8\pi G}{3}\rho R^2 = -kc^2\,. \tag{3.2}$$

We see the curvature term k returning in this formula. What becomes obvious is that for a specific density the universe will be flat. If the density is equal to

$$\rho_c = \frac{3H^2}{8\pi G}\,, \tag{3.3}$$

where $H = \dot{R}/R$, the universe is flat. This density is called the critical density. Often, densities are expressed as fraction of the critical density with a density parameter

$$\Omega = \frac{\rho}{\rho_c}\,. \tag{3.4}$$

If $\Omega = 1$, then the universe is flat. Inflation is requires a state that is driven by a negative pressure, this negative pressure is provided by the vacuum energy. Whereas the matter density falls off with $\rho_m \propto R^{-3}$, and the radiation density scales as $\rho_r \propto R^{-4}$, the energy density of the vacuum ρ_Λ is constant. We see that if we take equation (3.2), and we divide it by R^2, we obtain

$$H^2 - \frac{8\pi G}{3}\rho = \frac{-kc^2}{R^2}\,. \tag{3.5}$$

If we look at inflation, the vacuum energy dominates, so we assume that $\rho = \rho_\Lambda$, which is constant. This is called a de Sitter space. If we greatly increase R, while keeping H fixed, we see that the right hand side becomes negligible. We then end up with the following differential equation

$$\dot{R} = \sqrt{\frac{8\pi G\rho_\Lambda}{3}}R\,. \tag{3.6}$$

The solution to this equation is then an exponential:

$$R \propto e^{\bar{H}t} \text{ with } \bar{H} = \sqrt{\frac{8\pi G\rho_\Lambda}{3}}\,. \tag{3.7}$$

We see that the universe expands exponentially during the inflationary era. The reason we give this treatment of inflation will become clear in the next chapters, when we discuss production mechanisms of dark matter. If dark matter particles are created before, or during inflation, the exponential growth of the universe can decrease the density by such large amounts that we would see none of these particles today.

3.1.1 Second Friedmann equation

There is a second Friedmann equation, which is derived from different components of the Einstein field equations than equation (3.2). This equation is of the form of [10]

$$\ddot{R} = -\frac{4\pi GR(\rho c^2 + 3p)}{3c^2}\,. \tag{3.8}$$

We know from equation (3.7) that R grows exponentially, which means that the rate of expansion grows over time. Differentiating equation (3.7) gives us back the same equation for $\dot{R}$, only with a factor α in front of it. Thus we know that $\ddot{R}$ must have a positive sign. The only way we can obtain a positive sign on the right hand side is if the term containing the density and pressure is negative. We thus require that

$$\rho c^2 + 3p < 0\,. \tag{3.9}$$

3.1.2 Inflaton field

During inflation we have a scalar field ϕ with potential $V(\phi)$, called the inflaton field, that acts as the vacuum energy.

For inflation to take place, the value of the inflaton field ϕ should be larger than the Planck mass M_p of $\sim 10^{19}\,\text{GeV}$. During inflation, the value of ϕ starts out at a value larger than M_p, but it will decrease eventually and drop below $\sim M_p/3$, and the inflationary period ends [18]. What happens next is that ϕ will "roll down" the potential and start oscillating around the minimum of $V(\phi)$.[1] We have now entered the reheating phase. As we will show in section 3.2, ϕ behaves like a damped oscillator and will increase the temperature of the universe. We will also show that a scalar field ϕ can have a negative pressure required for inflation.

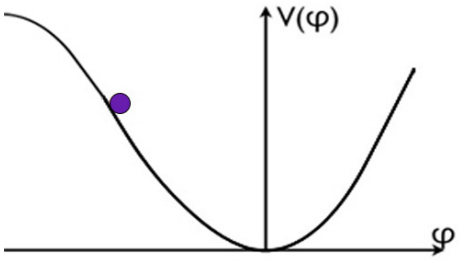

Figure 3.1: In this figure ϕ can be seen "rolling down" the inflaton potential. ϕ will oscillate around the minimum of the potential, which looks like a simple quadratic potential.

3.2 Scalar field dynamics

For a scalar field, the Lagrangian is of the form

$$\mathcal{L} = \frac{1}{2}\partial_\mu\phi\partial^\mu\phi - V(\phi) \tag{3.10}$$

.

where $V(\phi)$ is a potential depending on ϕ only. The action is then given by

$$S = \int \mathcal{L}\sqrt{-g}\; d^4x\,, \tag{3.11}$$

where for a homogeneous, isotropic universe (FLRW-model) $\sqrt{-g} = R^3(t)$, since we have to deal with an expanding universe. Using the principle of least action, the dynamics of this field follow from the Euler-Lagrange equations,

[1] It should be noted that if ϕ is in a false vacuum state, it might tunnel into the true vacuum state. If this happens, the region of space where the field is in the true vacuum state expands causally, while outside of this bubble inflation still takes place and space expands exponentially. This is also called the graceful exit problem.

$$\partial_\mu \frac{\partial(\mathcal{L}R^3(t))}{\partial(\partial_\mu\phi)} = \frac{\partial(\mathcal{L}R^3(t))}{\partial\phi}\,, \tag{3.12}$$

$$R^3(t)\ddot{\phi} + 3R^2(t)\dot{R}(t)\dot{\phi} - R^3(t)\nabla^2\phi = -R^3(t)\frac{\partial V}{\partial\phi}\,. \tag{3.13}$$

Again using the Hubble constant $H = \dot{R}/R$, this can be cast into the form,

$$\ddot{\phi} + 3H\dot{\phi} - \nabla^2\phi + \frac{\partial V}{\partial\phi} = 0\,. \tag{3.14}$$

The $3H\dot{\phi}$ term is called the Hubble drag term and has the form of a friction term. As mentioned, the period of inflation takes place when $\phi \gtrsim M_p/3$. If the field ϕ is coupled to a matter field, one can add an extra term $\Gamma\dot{\phi}$, resembling a friction term, representing particle creation [10], with Γ the rate of particle production. We can see from equation 3.15 that the oscillation of ϕ becomes more strongly damped if Γ increases. This is because the energy needed to create particles is taken from the inflaton field. If we additionally assume that the oscillations of ϕ take place in a harmonic potential $V(\phi) = \frac{1}{2}m^2\phi^2$, the equation of motion takes the following form

$$\ddot{\phi} + (3H + \Gamma)\dot{\phi} - \nabla^2\phi + m^2\phi = 0\,. \tag{3.15}$$

The oscillations of ϕ around the minimum of V will increase the temperature of the Universe and create new particles. This era is called the reheating phase. Since the universe expands with ~ 60 e-foldings during inflation, it is important that creation of super-heavy dark matter takes place after inflation has ended. As mentioned before, if this creation takes place during or before inflation, the density of the newly created particles will quickly drop as the universe rapidly expands.

3.2.1 Negative pressure

As mentioned in section 3.1.1, we will now show that the scalar field ϕ can indeed provide a negative pressure. For this we will start out from the energy-momentum tensor:

$$T^{\mu\nu} = \frac{\partial\mathcal{L}}{\partial(\partial_\mu\phi)}\partial^\nu\phi - \eta^{\mu\nu}\mathcal{L}\,, \tag{3.16}$$

where we will use the Lagrangian of equation (3.10). The density is defined as the time-time component of $T^{\mu\nu}$, i.e. T^{00}. The expression for the pressure is slightly more involved, $p = \left(T^{11} + T^{22} + T^{33}\right)/3$. These definitions give us

$$\rho = T^{00} = \frac{1}{2}\dot{\phi}^2 + \frac{1}{2}(\nabla\phi)^2 + \frac{1}{2}m^2\phi^2\,, \tag{3.17}$$

$$T^{ii} = \frac{1}{2}\dot{\phi}^2 + (\partial^i\phi)^2 - \frac{1}{2}m^2\phi^2 - \frac{1}{2}(\nabla\phi)^2\,, \tag{3.18}$$

which then allows us to calculate p

$$p = \frac{1}{2}\dot{\phi}^2 - \frac{1}{6}(\nabla\phi)^2 - \frac{1}{2}m^2\phi^2\,. \tag{3.19}$$

If we assume that during inflation the field is constant in both space and time, we have verified that $p = -\rho$, thus ϕ can provide a negative pressure needed for inflation.

Chapter 4

Creation of Dark Matter

There are several WIMP candidates for cold dark matter (CDM). These can be divided into two categories: thermal and non-thermal relics. The thermal relics were at some point in thermal equilibrium with the rest of the Universe, whereas non-thermal relics had little interaction, or their mass was too large to allow for creation of these particles [17]. In this chapter we will look at thermal production of dark matter, and a non-thermal mechanism called instant preheating. We require that the mechanism of dark matter creation is a mechanism that takes place after inflation. If such a model would predict dark matter creation before or during inflation, the resulting density of dark matter would be very low.

As discussed in chapter 2, candidates for non-thermal DM are most likely weakly interactive massive particles, also called WIMPS. The existence of SHDM was first theorised as an explanation for observations of ultra-high energy cosmic rays (UHECRs). If these SHDM particles have a mass in the range of $\gtrsim 10^{13}$ GeV, production of cosmic rays with ultra-high energies is possible upon annihilation or decay. As mentioned in section 1.2.1, cosmic rays with energies above 4×10^{19} eV can interact with CMB photons when travelling through space. In these interactions, the UHECRs lose energy. Thus cosmic rays from extra-galactic sources with sufficient energy to interact with the CMB are suppressed. Ultra-high energy cosmic rays must originate from a source at a distance of at most ~ 50 Mpc. Several possible mechanisms to create SHDM particles in the early universe have been proposed. These include [19]:

- Gravitational interactions from vacuum
- Thermal production during reheating
- Instant preheating, the decay of inflaton oscillations

The thermal production of SHDM particles requires an adequate temperature during the reheating phase in order to allow for the creation of super-heavy particles. The third method heavily depends on the coupling between the bosonic χ particle and the inflaton field ϕ, whereas in the first case no coupling is needed to produce particles. At instant preheating, oscillations of ϕ in the potential can create super-heavy bosons when ϕ is near zero. The mass of the created bosons is coupled to ϕ, and these bosons then decay into SHDM particles

when ϕ has come back to its maximum.

We will only briefly discuss gravitational production of dark matter here. In the early universe, fluctuations in the vacuum background of the universe can create particles. It is only the change in the metric of space that causes the production, no coupling to other fields is needed [19]. The particles created in this way can be sterile, i.e. they do not interact with other, but if they are unstable (with lifetime at least on the order of the age of the universe) their decay products could possibly be observed.

4.1 Thermal production

Thermal production of particles with $m \gtrsim 10^{13}$ GeV with correct numbers is in principle possible if the reheating temperature is in the range $10^{11} \lesssim T_r \lesssim 10^{15}$ GeV. Our thermal WIMP, X would then need to be coupled to, for example highly energetic photons or neutrinos,

$$X + \bar{X} \leftrightarrow \gamma + \gamma \,. \tag{4.1}$$

As long as the rate at which reactions happen is larger than the rate of expansion of the universe, that is

$$\Gamma\dot{\phi} \gtrsim H \,, \tag{4.2}$$

the particle density is at its equilibrium value. At a certain point the expansion of the universe wins and no more particles are created, the density now remains constant. This is called freeze-out.

4.1.1 Gravitino overproduction

Reheating temperatures in the range of $10^{11} \lesssim T_r \lesssim 10^{15}$ GeV or larger lead to the gravitino problem in supersymmetric models [20]. At high reheating temperatures, gravitinos will be overproduced. The decay of these particles will hinder the primordial nucleosynthesis in the early Universe. To avoid these problems, one should restrict oneself to temperatures $T_r \lesssim 10^9$ GeV, which do not allow for creation of superheavy WIMPS.

4.1.2 Thermal cross-section

For thermal DM, the current density is determined by the annihilation cross section. The larger the cross section, the easier it interacts and the longer it stays in equilibrium. The freeze-out density is inversely proportional to the annihilation cross section of the particle, $\Omega \propto 1/\sigma_{ann}$ [21]. Assume that our thermal WIMP is chargeless (else one could observe electromagnetic signals), and is allowed to couple to the weak interaction, the annihilation process given in figure 4.1 could be possible.

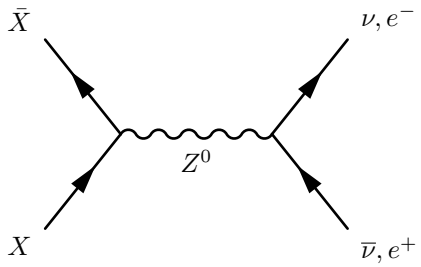

Figure 4.1: Possible annihilation process of thermally produced dark matter trough the weak interaction.

In the process a Z^0 boson is formed which then decays in to a fermion-antifermion pair, for example a neutrino-antineutrino or electron-positron pair. The amplitude of this process depends on the propagator of the Z^0 boson. Recall that the propagator for the Z^0 boson in this process is given by

$$\frac{g_{\mu\nu} - \frac{q_\mu q_\nu}{m_Z^2}}{q^2 - m_Z^2} = \frac{g_{\mu\nu} - \frac{q_\mu q_\nu}{m_Z^2}}{4m_X^2 - m_Z^2}\,, \tag{4.3}$$

where the q^2 is the four-momentum of the incoming particles squared. Since we are focusing on superheavy WIMPS as an explanation for UHECR, we would like to have particles with mass $\gtrsim 10^{13}\,\text{GeV}$. For these masses, the WIMP mass is many orders of magnitude larger than the mass of the Z^0 boson, so the term with m_X^2 dominates the propagator. This means the cross section for this process scales as

$$\sigma \propto m_X^{-2}\,. \tag{4.4}$$

Since the freeze-out density is inversely proportional to the annihilation cross section, the density of thermal WIMPS will scale with m_X^2 whenever $m_X \gg m_Z$, this gives quite a strong restriction to the maximum mass of thermal WIMPS of 100 GeV [17]. It is therefore highly unlikely that SHDM particles with mass $\gtrsim 10^{13}\,\text{GeV}$ are created by thermal processes.

4.2 Instant preheating

An interesting mechanism that can produce SHDM particles is the so-called 'instant preheating'. In this section an overview of this mechanism will be given. In short this mechanism depends on different couplings initially between the inflaton field ϕ and a scalar field χ. From these interactions bosons are created with mass m_χ^{eff}, where the mass of these bosons depends on ϕ. This allows for efficient particle creation during oscillations of ϕ, when ϕ is near zero [18]. As ϕ then increases, m_χ increases, the particles take up energy from ϕ. When ϕ reaches its maximum around $\sim 10^{-1}M_p =\sim 10^{18}$ GeV, the now very heavy (up to $\sim 10^{-1}M_p$ GeV depending on the strength of the interaction) χ-bosons can decay into a pair of ψ-fermions. It is these fermions that then are a candidate for SHDM and their annihilation should cause UHECR. In short, the different stages are

$$\phi \to \chi \to \psi + \bar{\psi}\,. \tag{4.5}$$

One can create particles from the oscillations of the inflaton field if the field of a particle, χ, is coupled to the inflaton field. In this scenario, we will consider a

quadratic potential $\frac{1}{2}m^2\phi^2$ as the potential of the inflaton field, and the interaction term between the ϕ and χ is $-\frac{1}{2}g^2\phi^2\chi^2$, where g is the coupling constant for this interaction. We have also included the interaction term $h\bar{\psi}\psi\chi$ which gives couples the χ and ψ particles. The Lagrangian for such a system is

$$\mathcal{L} = \frac{1}{2}\partial_\mu\phi\partial^\mu\phi - \frac{1}{2}m^2\phi^2 + \frac{1}{2}\partial_\mu\chi\partial^\mu\chi - \frac{1}{2}m_\chi^2\chi^2 + \frac{1}{2}g^2\phi^2\chi^2 - h\bar{\psi}\psi\chi\,. \quad (4.6)$$

A typical value for the inflaton mass in these models is $m = 10^{-6}M_p$, which is derived from CMB anisotropy measurements [22]. As mentioned before, the inflaton field behaves like a damped oscillator. We start out at the value of $\phi = M_p/3$, as instant preheating takes place right after inflation has ended. As mentioned before, inflation ends when ϕ drops below $M_p/3$. Thus after inflation has ended, ϕ behaves on short timescales as

$$\phi \approx \frac{M_p}{3}\frac{\sin(mt)}{mt}\,. \quad (4.7)$$

We will later show that this approximation for short time-scales is valid, since we only need to take the first 'swing' of ϕ into account. In the case that the mass of χ is nonzero if $\phi = 0$, and the particle has a 'bare mass' m_χ, one can show that χ obeys [22]

$$\ddot{X}_k + \left(\frac{k^2}{a^2} + m_\chi^2 + g^2\phi^2(t)\right)X_k = 0\,, \quad (4.8)$$

where $X_k = a^{3/2}\chi_k$. This enables us to get rid of the Hubble term containing $\dot{\chi}_k$. In this equation of motion the effective mass of χ is then given by $m_{\chi\ \mathrm{eff}}^2 = m_\chi^2 + g^2\phi^2(t)$. If we assume the bare mass m_χ is is small compared to the effective mass, $m_\chi^{\mathrm{eff}} \approx g|\phi|$, this mass changes in time as

$$|\dot{m}_\chi^{\mathrm{eff}}| = g|\dot{\phi}|\,. \quad (4.9)$$

At the end of inflation, ϕ starts to decrease from $\Phi \sim 10^{-1}M_p$, initially $|\dot{\phi}|$ is small and the process is adiabatic.
It is essential to note that the system initially changes adiabatically. Only if the effective mass changes rapidly enough, as we will show later, the system enters the non-adiabatic regime and particle creation can take place. Initially, ϕ has not yet rolled down much and therefore m_χ changes only slowly, following the expression given in equation (4.9).

We can illustrate the concept of adiabacity by taking a quantum harmonic oscillator in one of its eigenstates. If we very slowly change the spring constant, the shape of the potential will change, and so will the eigenstates of the system. Our wave function, which was originally in an eigenstate, will have evolved slowly to a the eigenstate of the new system with the same quantum numbers, i.e. if our wave function started out in the ground state, it will be in the ground state of the new potential. In this case, the change of the potential was adiabatic. If we would change the potential very rapidly, our wave function, which was in an eigenstate of the old potential, is now suddenly in a linear superposition of eigenstates of the new potential, amongst which possibly eigenstates with (much) larger energy.

This system loses its adiabacity when the rate of change of m_χ becomes larger than m_χ^2 [18], in other words when $g|\dot{\phi}| \gtrsim m_\chi^2$ or $|\dot{\phi}| \gtrsim g\phi^2$. The maximum value $\dot{\phi}$ can attain, which is at the center of the potential, is $\dot{\phi}_{\max} = m\Phi$, with $m = 10^{-6}M_p$ as before [22]. This maximum value for $\dot{\phi}$ gives an upper bound on the non-adiabatic regime, namely

$$g\phi^2 \lesssim |\dot{\phi}| \tag{4.10}$$

$$|\phi| \lesssim \sqrt{\frac{m\Phi}{g}} \tag{4.11}$$

$$|\phi| \lesssim 10^{-2}M_p\,. \tag{4.12}$$

We denote the value of ϕ at the transition between the adiabatic and non-adiabatic regimes by $|\phi_a| = 10^{-2}M_p$. In order for efficient particle creation using this mechanism, $g \gtrsim 10^{-4}$ [18]. The time in which this process happens is the time it takes for ϕ to roll from $-\phi_a$ to ϕ_a, which is approximately

$$t_a \approx \frac{|\phi_a|}{\dot{\phi}_{\max}} \sim (gm\Phi)^{-1/2} \sim 10^5 M_p^{-1}\,. \tag{4.13}$$

The typical momenta of the produced particles is $k_\star \sim t_a^{-1} \sim (gm\Phi)^{1/2}$. The particles are produced in a very short window of time.[1] After ϕ has crossed the non-adiabatic regime and increases to $\sim 10^{-1}M_p$, the effective mass of the χ particles starts to increase, until $m_{\chi\ \text{eff}} \sim g10^{-1}M_p$, assuming that the bare mass m_χ is at most on the order of $g|\phi|$. We will show in chapter 5 that the number of particles created is exponentially supressed for higher bare masses. If the χ bosons can have interactions with fermionic particles ψ via the term $h\bar{\psi}\psi\chi$ in the Lagrangian, the decay rate of χ particles is given by [22]

$$\Gamma(\chi \to \psi\bar{\psi}) = \frac{h^2 m_{\chi\ \text{eff}}}{16\pi}\left[1 - \left(\frac{2m_\psi}{m_{\chi\ \text{eff}}}\right)^2\right]^{\frac{3}{2}}\,. \tag{4.14}$$

From this equation it is easily seen that the decay is only allowed for $m_{\chi\ \text{eff}} > 2m_\psi$. Since the effective mass of the χ boson depends on ϕ, the largest decay rate occurs when ϕ reaches its maximum, at that point ψ fermionic pairs are created. In this way, the mechanism described here is very efficient in creating super-heavy particles.

[1] This would correspond to a time of $\sim 10^{-37}$ seconds.

Chapter 5

Particle density

Now that we have explained the mechanisms involved in the creation, it may be good to look at the number of particles that can be produced in this process. As crucial as it is to have a mechanism to create super-heavy particles, the mechanism should create them in the right amount, $\Omega \sim 0.3$. Too few WIMPS and these particles can only form a tiny fraction of the dark matter density, too many and they will overclose the universe.

We will first discuss the manner in which χ bosons are created in interactions with the inflaton field ϕ. We repeat equation (4.8)

$$\ddot{X}_k + \left(\frac{k^2}{a^2} + m_\chi^2 + g^2\phi^2(t)\right) X_k = 0 \tag{5.1}$$

$$\ddot{X}_k + \omega^2 X_k = 0\,. \tag{5.2}$$

In the adiabatic regime which was discussed in section 4.2, the solution to this equation can be written as a linear superposition of an incoming and an outcoming wave with coefficients $\alpha_k(t)$ and $\beta_k(t)$ [23].

$$X_k(t) = \frac{\alpha_k(t)}{\sqrt{2\omega}} e^{-i\int \omega\, dt} + \frac{\beta_k(t)}{\sqrt{2\omega}} e^{i\int \omega\, dt} \tag{5.3}$$

At $t = 0$, $\alpha_k = 1$ and $\beta_k = 0$. The occupation number for a certain value of k is given by $n_k = |\beta_k|^2$. But in the region $|\phi| \lesssim \sqrt{m\Phi/g}$ where ϕ behaves non-adiabatically, this solution breaks down. If ϕ passes through the non-adiabatic regime at a time t_j, we denote the wave $X_k(t)$ just before this time by $X_k^j(t)$ with coefficients α_k^j and β_k^j. When the wave has left the non-adiabatic regime, we denote this with a label $j+1$ instead of j. The wave scatters around the minimum of the potential in the non-adiabatic regime. The incoming amplitudes α_k^j, β_k^j are related to the outgoing amplitudes α_k^{j+1}, β_k^{j+1} by the following equation

$$\begin{pmatrix} \alpha_k^{j+1} e^{-i\theta_k^j} \\ \beta_k^{j+1} e^{i\theta_k^j} \end{pmatrix} = \begin{pmatrix} \frac{1}{D_k} & \frac{R_k^\star}{D_k^\star} \\ \frac{R_k}{D_k} & \frac{1}{D_k^\star} \end{pmatrix} \begin{pmatrix} \alpha_k^j e^{-i\theta_k^j} \\ \beta_k^j e^{i\theta_k^j} \end{pmatrix}. \tag{5.4}$$

R_k is the reflection, and D_k is the transmission parameter. Also appearing is the phase $\theta_k^j = \int_0^{t_j} \omega\, dt$ the wave has when entering the non-adiabatic regime.

The reflection and transmission parameters can be obtained by rewriting equation (5.1) with $\phi(t)$ approximated around t_j as $\phi(t) \approx (t-t_j)^2$ and $k_\star = \sqrt{mg\Phi}$ from section 4.2. Introducing variables $\tau = k_\star(t-t_j)$ and $\kappa^2 = \frac{k^2/a^2+m_\chi^2}{k_\star^2}$, we can write

$$\frac{d^2X_k}{d\tau^2} + (\kappa^2+\tau^2)X_k = 0\,. \tag{5.5}$$

The solutions of this equation determine R_k and D_k. This allows us to determine $n_k^{j+1} = |\beta_k^{j+1}|$, the number of particles after the scattering. If we start out with $n_k^j = 0$, as we do not have any χ particles before ϕ enters the non-adiabatic regime. Using equation (5.4) to determine $n_k^{j+1} = |\beta_k^{j+1}|$ gives the number of particles with momentum k as [23]

$$n_k = e^{-\pi\kappa^2}\,. \tag{5.6}$$

Filling in the expression for κ^2 and $k_\star$, we obtain

$$n_k = \exp\left(-\frac{\pi\left(k^2+m_\chi^2\right)}{mg\Phi}\right)\,. \tag{5.7}$$

We have set $a^2 = 1$, this term is related to the expansion of the universe, and by setting this to zero, we do not take into account effects due to expansion of the universe. The time ϕ is in the non-adiabatic regime is very short: $\sim 10^{-37}$ s, which allows us to safely make this assumption. The expression n_k gives the number of particles occupying a state with momentum k. We can determine the total number density of χ particles by integrating over the possible momentum states, using n_k from equation (5.7),

$$n_\chi = \frac{1}{(2\pi)^3}\int d^3k\; n_k\,. \tag{5.8}$$

By making a switch to spherical coordinates we get

$$n_\chi = \frac{1}{(2\pi)^3}\int_0^\infty dk\; 4\pi k^2 n_k \tag{5.9}$$

$$n_\chi = \frac{(mg\Phi)^{3/2}}{(2\pi)^3}\exp\left(-\frac{\pi m_\chi^2}{mg\Phi}\right)\,. \tag{5.10}$$

From this formula one can clearly see that the production of particles with $m_\chi^2 \gtrsim mg\Phi$ is heavily suppressed. Let us now look at the case $m_\chi^2 \lesssim mg\Phi$. The energy density of these particles is given by

$$\rho_\chi = n_\chi m_\chi^{eff} \sim \frac{m^{3/2}(g\Phi)^{3/2}\,(m_\chi+g\phi)}{(2\pi)^3}\exp\left(-\frac{\pi m_\chi^2}{mg\Phi}\right) \tag{5.11}$$

$$\approx \frac{m^{3/2}(g\Phi)^{5/2}}{(2\pi)^3}\exp\left(-\frac{\pi m_\chi^2}{mg\Phi}\right)\,. \tag{5.12}$$

The last equation holds when ϕ is close to Φ so that $m_\chi \ll g\Phi$, and $m_\chi^{eff} \approx g\Phi$. Let us now compare ρ_χ to the energy density of the inflaton field, ρ_ϕ. Recall

that the energy momentum tensor is given by

$$T^{\mu\nu} = \frac{\partial \mathcal{L}}{\partial(\partial_\mu \phi)} \partial^\nu \phi - \eta^{\mu\nu} \mathcal{L} \,. \tag{5.13}$$

To obtain the energy density, we need to calculate T^{00}.

$$\rho_\phi = T^{00} = \frac{1}{2}\dot{\phi}^2 + \frac{1}{2}(\nabla\phi)^2 + V(\phi) + \frac{1}{2}g^2\phi^2\chi^2 \tag{5.14}$$

Where the Lagrangian from equation 4.6 was used with potential $\frac{1}{2}m^2\phi^2$ and including the interaction term $-\frac{1}{2}g^2\phi^2\chi^2$. Assuming the energy density does not change too much if ϕ changes, we can say that

$$\rho_\phi \sim \frac{1}{2}(m\Phi)^2 \,. \tag{5.15}$$

From equations (5.11) and (5.15) the ratio between ρ_χ and ρ_ϕ is

$$\frac{\rho_\chi}{\rho_\phi} \sim \frac{m^{-1/2}\Phi^{1/2}g^{5/2}}{16\pi^3} \,. \tag{5.16}$$

We take the value $g \sim 10^{-4}$, which is the minimal value needed for efficient preheating. If we also assume $\Phi \sim 0.1 M_p$, the energy density of the newly created particles is

$$\rho_\psi = \rho_\chi \sim 10^{97} \exp\left(-\frac{\pi m_\chi^2}{10^{-11}M_p^2}\right) \mathrm{GeV}\, m^{-3} \,. \tag{5.17}$$

This gives a value of $\rho_\chi \sim 10^{97}\,\mathrm{GeV}\, m^{-3}$ for the energy density if $m_\chi^2 \lesssim mg\Phi$. The value of the exponent in this case lies within one order of magnitude of unity, thus we ignore it in this regime. The χ particles of course decay into ψ bosons, but that does not change the energy density.

5.1 Density evolution

If $m_\chi^2 \sim mg\Phi$, then one might think that the energy density is off by a huge amount. Partly this is because we did not yet take the expansion of the universe into account. The end of inflation, the time when instant preheating takes place, lies at a redshift of $z \sim 10^{22}$ [1] The density of matter in the universe changes with the inverse of the scale factor cubed, $\rho_m \propto a^{-3}$. The current energy density of dark matter would be a factor 10^{66} lower than right after inflation and thus

$$\rho_\chi \sim 10^{33} \exp\left(-\frac{\pi m_\chi^2}{10^{-11}M_p^2}\right) \mathrm{GeV}\, m^{-3} \,, \tag{5.18}$$

which is still way too high if $m_\chi^2 \sim mg\Phi$. If we want to obtain the correct current density, we should look at a particle with a slightly higher bare mass.

[1] This can be calculated from the ratio between the current temperature of the universe $T_0 = 2.73K \sim 10^{-13}$GeV and the temperature at reheating, where $T_R \sim 10^9 GeV$ is a reasonable value, see [20], which takes place directly after the instant preheating. Since $z \propto a$ and $T \propto a^{-1}$, we can easily make an estimate of the redshift at the time of instant preheating.

The dependence on the bare mass m_χ is very steep, with the energy density dropping a few orders of magnitude even for a slight increase of the mass. To get a density of $\rho_\chi \sim 1\,\mathrm{GeV}\,m^{-3}$, we find that the mass of the χ bosons at their decay can range from $10^{14}\,\mathrm{GeV}$ for $g \sim 10^{-4}$ to $10^{18}\,\mathrm{GeV}$ for $g \sim 1$. This means that each of the two ψ can have mass $m_\chi/2$ and that m_ψ can also be on the order of 10^{14} GeV to 10^{18} GeV.

5.1.1 First swing

But wait, we only took into account the first swing of ϕ. Surely ϕ will eventually pass its minimum again and create more particles? Wouldn't that affect the density too? The short answer is no, but let's motivate this answer. The ratio of particles created in the second and first swing is

$$\frac{n_\chi^{(2)}}{n_\chi^{(1)}} = \left(\frac{1}{2}\right)^{3/2} \exp\left(-\frac{3\pi^2 m_\chi^2}{gmM_p}\right) . \tag{5.19}$$

The derivation of this formula is given in appendix A. For the values used and obtained in the previous section the resulting ratio is

$$\frac{n_\chi^{(2)}}{n_\chi^{(1)}} \sim 10^{-13} . \tag{5.20}$$

The later swings will be suppressed even more, so we can indeed only consider the first swing of ϕ.

5.2 SHDM lifetime

In calculating the density evolution of χ, we only took the expansion of the universe into account. What we did not take into account was the decay of the SHDM. The implicit assumption was made that the lifetime of the ψ fermions is at least comparable to the age of the universe $\tau \gtrsim 10^{10} yr$. If the lifetime is already an order of magnitude smaller than this age, there would be a large abundance of energy of decay products of the SHDM. We will therefore require that these particles are metastable, their lifetime is at least on the order of the life of the universe [24].

If we assume the ψ particles are allowed to decay, then along the decay process emission of photons will take place. The decay products created from these decays in the hadronic jet are dominated by pions (90%) [25], and thus UHECRs will mostly consist of the decay products of pions. The observed photon flux can give an estimate of the lifetime of SHDM. Starting from the decay of uniformly distributed dark matter, the flux is given by [24]

$$J_\gamma = \frac{1}{4\pi} l(E_\gamma) \dot{n}_\psi \frac{dN_\gamma}{dE_\gamma} . \tag{5.21}$$

The attenuation length is taken to be $l(E_\gamma) = 10$ Mpc and $\frac{dN_\gamma}{dE_\gamma} \approx E_\gamma^{-1.5}$ [24]. We have to follow a slightly different analysis, since we know that dark matter is not distributed uniformly throughout the universe, but rather it is clumped into

halos [26] around galaxies and galactic clusters. This gives slight modifications to the relation between the lifetime and mass of the particle, namely [22]

$$\tau_\psi = 3.16 \times 10^{18} f(\Omega_\psi h^2) \left(\frac{M_p}{m_\psi}\right)^{1/2} . \tag{5.22}$$

In the above formula, f is a factor related to the distribution of dark matter. It is the ratio between the galactic and extra-galactic flux, $f = J_H/J_{\text{ex}} = n_H R_H/nl(E_\gamma)$ [25, 24]. It is 1 for a uniform distribution, but in case the WIMPs are clustered in a galactic halo, $f \approx 10^3$. For the same mass range of $10^{14} \lesssim m_\psi \lesssim 10^{18}$ GeV, the lifetime ranges from 10^{23} to 10^{21} yr. Super-heavy WIMPs are able to survive long enough. Their lifetime is well above 10^{10} yr, and dark matter formed in the early universe will therefore not have decayed since then.

5.3 Annihilation

There is also the possibility that the ψ particles cannot decay, but that they only can annihilate. Since the ψ particles are created in pairs from the decay of the χ bosons, the ψ particles could form a χ boson when annihilating. Since χ cannot couple directly to normal matter, else formation of ψ particles would be very unlikely seen their mass, the decay possibly takes place via a coupling to the inflaton field. If this is the case then a possible way in which the particles can annihilate is:

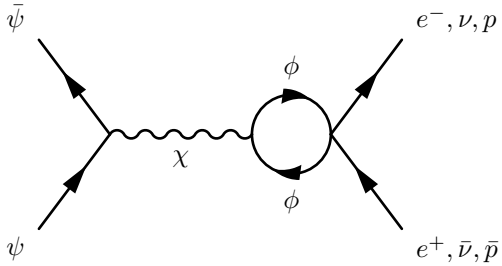

Figure 5.1: Possible annihilation reaction of ψ particles

This requires the inflaton field to be coupled to normal matter fields, so that for example electron or neutrino pairs could be produced with very high energies. One could also expect that in the annihilation process pions are formed, which could produce ultra-high energy photons in their decay.

Chapter 6

Dark Matter halos

As mentioned before, UHECRs with energies above the GZK cutoff should come from the neighbourhood of our Earth, at least within a distance of 100 Mpc. Like ordinary matter, dark matter is also subject to gravity and will form halos around the (large scale) structures in the universe like our galaxy or in clusters of galaxies. This section aims to discuss whether annihilation processes inside these halos, in particular the dark matter halo of our own galaxy, can produce UHECRs.

Small quantum fluctuations during the inflationary epoch give the initial conditions for the formation of cosmic structure formation. In this process, the present dark matter also follows this pattern and starts clustering around ordinary matter. In this section we will focus on the distribution of dark matter around galaxies. In current standard cosmology, cosmic structure formation is dominated by cold dark matter (CDM). Cold means here that the dark matter particles move at non-relativistic velocities. CMD allows for structure formation for small structures with masses even below one solar mass [26]. In particular, cosmic structure formation in the universe starts with the formation of smaller structures with masses comparable to Earth [27].

From simulations and observations [26, 28], the current distribution of dark matter in galaxies and clusters is given by a so-called dark matter density profile [29]. This density distribution in its most general expression takes the form

$$\rho(r) = \frac{\rho_s}{(r/r_s)^\gamma (1 + (r/r_s)^\alpha)^{(\beta-\gamma)/\alpha}} \,. \tag{6.1}$$

For $\alpha = 1$, $\beta = 3$ and $\gamma = 1$ this is equal to the Navarro-Frenk-White (NFW) profile [28]. r_s and ρ_s are respectively the scale radius and density, which are characteristics of an individual halo. One could naively extend this formula to very large r, since there is no clear point where the halo suddenly ends. Therefore, it is imperative to make a clear distinction between matter that does and does not belong to the halo. Following the existing literature [26, 28], we will define the extent of the dark matter halo to be the region where the density of dark matter ρ_{DM} has an overdensity of at least 200 times the background density, the average matter density ρ_M in the universe.

6.1 Subhalos

From the GHALO and the Via Lactea II simulations [26, 28, 30] substructures in the larger halo were resolved. These simulations start from initial conditions based on the results of WMAP. In for example the GHALO simulation, around $\sim 10^5$ subhalos could be identified from the main halo structure within the virial radius [30]. These subhalos are created when smaller halos fall into the larger main halo. The outer parts of this smaller halo are ripped apart by tidal forces but the central denser part survives and forms the subhalo. The radius of a subhalo is defined to be the radius where the density of the subhalo becomes equal to that of the host halo.

It is worth noting that the subhalos follow the same structure as the main halo, they contain subhalos too, in this case called subsubhalos. This pattern goes on down to the CDM cut-off scale, which can be as low as a single Earth mass. The different levels of subhalos have been called sub^{n}halos [28]. Also, the central parts of subhalos can survive inside the host halo, thanks to their large density. It was also found that density profiles of subhalos are similar to that of their host halo [26], but there are some differences. The DM density in subhalos generally falls of quicker for larger radii, which is what one would expect if the outer parts of the halo are stripped away.

The distribution of dark matter in a galactic halo does therefore not follow a smooth profile. In the inner region the distribution of dark matter is smooth [28], but further outside the density profile becomes bumpy as the contributions of subhalos and regions with smaller densities gets larger.

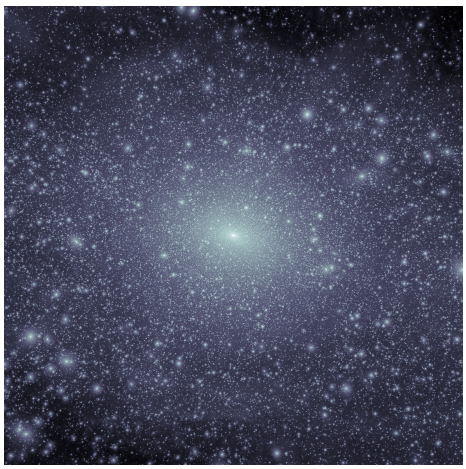

Figure 6.1: Result from the VL-II simulation [31]. The figure shows the dark matter density in a 800kpc square. Inside the main halo, smaller subhalos are visible as small clumps.

6.2 Dark Matter annihilation in halos

Indirect detection of dark matter depends on the detection of γ rays or neutrinos produced in decays or annihilation processes of dark matter. We already discussed the lifetime of the SHDM before, placing it in the range of 10^{21} to 10^{23} yr, depending of the mass of our ψ particles. In this section we will look at annihilation processes. Detection of annihilation products of SHDM in the form of ultra-high energy cosmic rays is crucial to the indirect detection of these very massive WIMPS.

In chapter 5 we briefly discussed a possible annihilation reaction. The key issue was that when a pair of ψ particles annihilate and form a χ boson, this χ boson should not directly couple to ordinary particles, otherwise it would have decayed into these particles before it could decay into much more massive ψ pairs. To circumvent this problem, a process seen in figure 5.1 on page 20 could be a plausible process. The most likely candidates for detection would be neutrally charged particles, since they do not interact with the galactic magnetic field and can travel a longer distance through the galaxy.

The main reason why we have looked at substructure of galactic halos is to look at possible sources of ultra-high energy cosmic rays. The sub^{n}halos are of interest because they form superdense clumps inside the host halo. The annihilation rate, and thus the luminosity from annihilation scales as

$$L \propto \rho^2 \,. \tag{6.2}$$

In simulations, the contribution from the subhalos that could be resolved to the total luminosity was approximately equal to the luminosity of the main halo [26]. The substructure of the main halo thus gives a 'boost' to the luminosity of dark matter annihilation reactions. We can define a boost factor

$$B = \frac{L_{\text{total}}}{L_{\text{main halo}}} \,. \tag{6.3}$$

This boost factor was around two in simulations [27, 30], but both simulations were naturally constrained by their resolutions. Extrapolations for the contribution of even smaller scale sub^{n}halos raise the boost factor to $B = 16$ [26]. This extrapolation hints that signals from the annihilation of SHDM largely originate from small subhalo clumps in the main galactic halo.

6.3 Anisotropy

Crucial to the top-down model of annihilating SHDM is the arrival direction of the signals from SHDM annihilation. Ultra-high energy cosmic rays with energies above the GZK cut-off should come from within a distance of ~ 50 Mpc. This would mean that observed GZK cosmic rays are likely to originate from our galaxy. As we explained in the previous section, dark matter annihilation is much more likely in the denser parts of the dark halo, see equation (6.2). Therefore, this model predicts that the arrival direction of highest-energy cosmic rays follows the dark matter density distribution. Even if the boost factor from sub^{n}halos is raised to 16, the contribution of a single subhalo is small because of

the large abundance of subhalos and their smaller size compared to the host halo. More extended regions of higher density like the core of the dark halo should be noticeable in the arrival direction pattern. This model therefore predicts an anisotropy for cosmic rays above the GZK cut-off. Observation of such an anisotropy would strengthen the super-heavy dark matter scenario.

6.3.1 Extragalactic anisotropy

Dark matter is not only present in our galaxy, other galaxies have dark halos too. Dark matter annihilation in these halos can give ultra-high energy cosmic rays from an extragalactic source. These cosmic rays can travel a maximal distance of ~ 50 Mpc. This is slightly less than the size a supercluster can have, around $100h^{-1}$ Mpc [32]. Our galaxy is part of the Local Group, which is in turn part of the Virgo Supercluster, centered around the Virgo cluster, which lies around ~ 17 Mpc from our galaxy [33]. Thus, ultra-high energy cosmic rays from annihilation in the dark halos of other galaxies in the supercluster are able to reach us.

If these extra-galactic ultra-high energy cosmic rays form a large fraction of the cosmic ray flux, then we might see a correlation between the arrival directions and the matter distribution in nearby clusters. Dark matter and baryonic matter are both subject to gravity, therefore their distributions are similar. It has been proposed in [33] that such a correlation is not present at GZK-energies due to diffuse propagation because of magnetic fields of $\sim 10^{-7} - 10^{-8}$ Gauss in the Virgo Supercluster. In this case, particles with an energy 10^{20} eV or above propagate in an almost straight line, and correlations with matter in the supercluster should become significant for these energies. This is however, very dependent on the strength of the intergalactic magnetic field, and recent observations from the Auger observatory [34] seem to indicate that the arrival direction of UHECRs is most likely isotropic.

6.4 Dark halo of the Milky Way

It has been suggested that for the Milky Way, the Burkert profile may fit the density profile of the galactic dark halo better [35]. This profile is of the form

$$\rho(r) = \frac{\rho_0}{(1 + r/R)(1 + (r/R)^2)} \,. \tag{6.4}$$

It contains a central density $\rho_0 = 4 \times 10^7$ $\mathrm{M}_\odot$ kpc^{-3} and a scale radius of $R = 9.26$ kpc [35]. The scale radius is the radius for which the density profile steepens, since now the $(r/R)^2$ term begins to play a role. In chapter 7 we will use this profile in our estimate of the annihilation cross section of SHDM.

Chapter 7

Annihilation cross section

In this chapter we make a rough estimate of the cross section of the annihilation process of two dark matter particles. The procedure in which we obtain the cross section is as follows. We start out by calculating the total flux cosmic rays with energies above 10^{12} eV. For this we will integrate the differential cosmic ray spectrum from 10^{12} eV to the knee at an energy of 5×10^{15} eV. Since the differential cosmic ray spectrum in this range scales is $\propto E^{-2.7}$, which becomes even steeper above the knee, the contribution of this part of the spectrum does not contribute much to the total flux, we will ignore this in our estimate here. We use this flux to make an estimate of the density of cosmic rays (which is assumed to be isotropic) in a sphere with a radius of 100 kpc around the centre of our galaxy.

Up until the energy of 5×10^{15} eV, cosmic rays can are trapped in the magnetic field of the galaxy, but eventually escape. Taking an average escape time, we can calculate the number of cosmic rays, and therewith the energy contained in these cosmic rays, that leaves the galaxy. If we assume that this flux is being kept constant by the creation of new cosmic rays, we can estimate the annihilation rate. Knowing the distribution of dark matter in the galaxy, we can infer the velocity averaged cross section $\langle \sigma v \rangle$ needed to sustain this flux. We will then interpret the result of the estimate.

7.1 Cosmic ray flux

From a primary energy of 10^{12} eV up to the knee at $\sim 5 \times 10^{15}$ eV the differential spectrum of cosmic rays can be described by

$$\frac{dF}{dE} = aE^{\gamma}\,, \tag{7.1}$$

where $\gamma = -2.7$ and $a = 1.3 \times 10^5$ in the energy range up to the knee. For energies above the knee the parameter γ decreases to -3.1, meaning the flux of cosmic rays falls off even quicker. To obtain the flux between $E_{\text{low}} = 10^{12}$ eV

and $E_{\text{knee}} \sim 5 \times 10^{15}$ eV we integrate equation (7.1) over this energy range

$$F = a \int_{E_{\text{low}}}^{E_{\text{knee}}} \frac{dF}{dE} dE \tag{7.2}$$

$$= \frac{a}{1+\gamma} \left(E_{\text{knee}}^{\gamma+1} - E_{\text{min}}^{\gamma+1} \right) \tag{7.3}$$

$$= 0.0588 \left(\text{m}^2 \text{sr s} \right)^{-1} . \tag{7.4}$$

To get the energy flux, we need to weigh the spectrum with a factor E, with the same boundaries as used in equation (7.2), resulting in the following integral

$$I = a \int_{E_{\text{low}}}^{E_{\text{knee}}} E \frac{dF}{dE} dE \tag{7.5}$$

$$= \frac{a}{2+\gamma} \left(E_{\text{knee}}^{\gamma+2} - E_{\text{min}}^{\gamma+2} \right) \tag{7.6}$$

$$= 142 \text{ GeV} \left(\text{m}^2 \text{sr s} \right)^{-1} . \tag{7.7}$$

To obtain the average the energy per cosmic ray we use

$$\langle E \rangle = \frac{I}{F} = 2423 \text{ GeV} . \tag{7.8}$$

We see that this average energy of the cosmic rays lies close to our lower integration bound. This is because the number of cosmic rays quickly decreases as with energy, see equation (7.1).

7.2 Cosmic ray density

We now know the flux of cosmic rays as measured on Earth, and we made the assumption that this flux is isotropic in a sphere with a radius of 100 kpc, centered at our Milky Way. We now have to relate the measured flux to a density of cosmic rays. If we know the density, we can extend this density and obtain the number of cosmic ray particles in our galaxy.

We measure a flux of $4\pi F = 0.74 \left(\text{m}^2 \text{ s} \right)^{-1}$, and we included a factor 4π to account for the fact that the flux was per steradian. We take our "detector", a sphere with radius r_0, such that its cross section has an area of $\pi r_0^2 = 1$ m^2. From a distance R, the chance that a particle flies through the detector is $\rho/(4\pi R^2)$, where ρ is the density of cosmic rays. Cosmic rays at these energies move close to the speed of light, so the maximum distance a cosmic ray can travel in a second is a lightsecond. The total amount of cosmic rays that flies through the detector is then given by

$$\int_{r_0}^{1 \text{ ls}} dR \, 4\pi R^2 \frac{\rho}{4\pi R^2} = \int_{r_0}^{1 \text{ ls}} \rho \, dR . \tag{7.9}$$

which should be equal to the measured value of $4\pi F$. Solving integral (7.9) and equating it to the measured flux gives

$$3 \times 10^8 \text{m} \, \rho = 4\pi F . \tag{7.10}$$

Filling in the number gives us the number density of cosmic rays

$$\rho = \frac{4\pi F}{3 \times 10^8} = \frac{0.74}{3 \times 10^8} \mathrm{m}^{-3} = 2.46 \times 10^{-9} \mathrm{m}^{-3} = 7.24 \times 10^{49} \mathrm{kpc}^{-3}\,, \quad (7.11)$$

where we have omitted r_0 since it is very small compared to a lightsecond. Multiplying this density with the volume of a sphere with radius 100 kpc gives us 3.03×10^{56} cosmic ray particles in and around the Milky Way.

7.2.1 Escaping cosmic rays

We will now calculate the amount of cosmic rays that escape the galactic magnetic fields. The cosmic rays are trapped in the magnetic field of the galaxy are not trapped forever. We assume that on average they have an average escape time of $\tau = 15 \times 10^6$ yr [36]. This means that if the current number of cosmic rays in the galaxy is N_0, over time this will decrease following

$$N(t) = N_0 e^{-t/\tau}\,. \quad (7.12)$$

The number of cosmic rays that escape at a certain time is given by

$$\dot{N} = \frac{-N_0}{\tau} e^{-t/\tau}\,. \quad (7.13)$$

This means the number of particles currently escaping is N_0/τ, meaning every second

$$\frac{3.03 \times 10^{56}}{\tau} = 6.41 \times 10^{41} \mathrm{s}^{-1} \quad (7.14)$$

cosmic rays escape the milky way with average energy $\langle E \rangle = 2423$ GeV. This means that the energy loss due to the escaped cosmic rays is

$$1.55 \times 10^{45} \mathrm{GeV\ s}^{-1}\,. \quad (7.15)$$

7.3 Cross section

We have calculated number of cosmic rays, and the energy that is lost due to the cosmic rays escaping the Milky Way. We will now look at the number of annihilations required to sustain this flux. In each annihilation of two particle with mass 10^{14} GeV, an amount of 2×10^{14} GeV of energy is released. Using the result (7.15) of the previous section, we would need an annihilation rate of

$$\frac{1.55 \times 10^{45} \mathrm{GeV\ s}^{-1}}{2 \times 10^{14} \mathrm{GeV}} = 7.76 \times 10^{30} \mathrm{s}^{-1}\,. \quad (7.16)$$

The rate of annihilation depends on the square of the local dark matter density and on the velocity averaged cross section $\langle \sigma v \rangle$. We integrate the square of the density over the volume of the 100 kpc^3 we introduced earlier. We thus have the relation

$$\int_{\mathrm{halo}} \frac{\rho_{\mathrm{dm}}^2}{m_\psi^2} \langle \sigma v \rangle dV = 7.76 \times 10^{30} \mathrm{s}^{-1}\,. \quad (7.17)$$

For the dark matter density profile ρ_{dm}, we take the Burkert density profile given in equation (6.4). To obtain a number density we have to divide the

density by the mass of the SHDM particle, hence the m_ψ^2 term in the integral. Solving the integral, the thermally averaged cross section is given by

$$\frac{1.8 \times 10^{18} \mathrm{M}_\odot^2}{m_\psi^2 \mathrm{kpc}^3} \langle \sigma v \rangle = 7.76 \times 10^{30} \mathrm{s}^{-1} \,. \tag{7.18}$$

The units here are slightly inconvenient, so we express the final value of the velocity average cross section as

$$\langle \sigma v \rangle \approx 1.08 \times 10^{-15} \mathrm{m}^3 \mathrm{s}^{-1} \,. \tag{7.19}$$

We can go one step further in our estimate. If the temperature of the dark halo is on the order of 1000 K, the average kinetic energy per particle is

$$\langle E_{\mathrm{kin}} \rangle = \frac{T}{k_B} = 86 \text{ meV} \,. \tag{7.20}$$

Since these heavy particles are cold dark matter, they move with velocities that are small compared to the speed of light. We can then use the simple formula

$$\langle E_{\mathrm{kin}} \rangle = \frac{1}{2} m_\psi \langle v \rangle^2 \tag{7.21}$$

to obtain an average velocity of $\langle v \rangle \approx 4 \times 10^{-4}$ m/s. Dividing equation (7.19) by this average velocity we obtain a cross section of

$$\sigma = \frac{\langle \sigma v \rangle}{\langle v \rangle} \approx 2.7 \times 10^{-12} \text{ m}^2 \,. \tag{7.22}$$

For a cross section this is a very large value. The obtained value must be seen an upper limit for the cross section of SHDM annihilation. As a sanity check, we calculated in appendix B that the ratio of annihilating particles to the total number of particles lies around

$$2 \times 10^{-24} \mathrm{s}^{-1} \,. \tag{7.23}$$

If the annihilation rate is constant for a time of 10 Gyr, then

$$2 \times 10^{-24} \mathrm{s}^{-1} \times 10 \mathrm{Gyr} \approx 6 \times 10^{-7} \tag{7.24}$$

of the particles in the dark matter halo have annihilated. This is a small fraction. This ensures that even for this large cross section, only a small part of the dark matter has annihilated.

7.3.1 Remarks to the estimated cross section

We will now look at some of the assumptions that were done in order to obtain an estimate for the annihilation cross section. We noticed is that our estimate for the cross section was very large.

Can there be certain factors that could result in a lower cross section? First of all, if we assume that the density of dark matter in the Milky Way is relatively well known, the best way to bring down the cross section is to provide plausible explanations that could lower the annihilation interaction rate. The first thing that comes to mind is that we have assumed that all cosmic rays are produced in the annihilation of SHDM. If the amount of cosmic rays due to dark matter annihilation only provides a minor part of the total cosmic ray flux, the expected cross section lies lower.

To be still able to provide an explanation for the origin of UHECRs, the energy spectrum should be different from the total energy cosmic ray spectrum. Consider that the flux of cosmic rays produced in SHDM annihilation is small for the lower energies, but that for these cosmic rays, the spectrum falls off less with energy. This way, the cosmic rays produced in SHDM annihilation could become the dominant source of cosmic rays only at the very highest energies.

Lastly, we assumed that all cosmic rays were due to annihilation of dark matter in our galaxy. If we would take into account dark matter annihilation in dark halos of galaxies and in clusters in our neighbourhood, the rate of annihilation inside the milky way would be lower. This would result in a lower value for the cross section.

Chapter 8

Conclusion and outlook

In order to explain detections of ultra-high energy cosmic rays with energies above the GZK cut-off, we have looked at annihilation of superheavy dark matter particles. To produce these cosmic rays by this mechanism requires that the mass of the SHDM particles is $\gtrsim 10^{13}$ GeV. We have looked into the production production mechanisms suited for creating these particles. It was found that these particles cannot be created by thermal processes, as this would limit the mass to a maximum of 100 TeV. We found that the instant preheating mechanism that creates SHDM pairs from decaying χ-bosons that are coupled to the inflaton field ϕ allows for the creation of particles in the range of 10^{13} to 10^{18} GeV. Relating the amount of particles created by this mechanism to the current observed dark matter content, we found that a mass on the order of 10^{14} GeV gives a density that is consistent these observations, if we assume the instant preheating is somewhat efficient. Increasing the coupling of χ to ϕ allows for even larger masses, up to 10^{18} GeV, one order of magnitude below M_p.

If the particles can decay, we found their lifetime lies in the range of 10^{21} to 10^{23} yr. This is much larger than the minimum lifetime we required, which was that the superheavy dark matter particles have lifetimes of at least the age of the universe. We then studied the annihilation process of dark matter. Dark matter is clustered around our galaxy in a halo. Simulations [26, 28, 30] showed that the dark halo does not follow a smooth profile, and revealed substructure in the form of smaller, dense clumps called subhalos. In general, the annihilation rate scales as ρ^2, meaning that dense clumps can give a boost to the total annihilation rate. The lower energy cosmic rays will generally have isotropic arrival directions, as they are trapped in the galactic magnetic field. For the higher energy cosmic rays, this model would predict a correlation of the arrival direction of cosmic rays the dark matter distribution in the galaxy. If the origin of UHECRs is predominantly extragalactic, then for energies above 10^{20} eV the arrival direction should be correlated with matter in our local Supercluster. Observation of such anisotropy can provide evidence for dark matter as source of (ultra-high energy) cosmic rays, but so far no anisotropy has been observed.

Finally we made an estimate of the cross section of SHDM annihilation interactions. The cross section of $\sigma \approx 2.7 \times 10^{-12}$ m^2 is very large, and in this regard should be seen as an strict upper limit on the SHDM annihilation cross section.

Outlook

Subjects that could be studied further are the annihilation mechanism of SHDM and the types of particles produced in this process. In particular interesting are the upper limits on the photon fraction of 2.0% at 10^{19} eV, to 31% at the cut-off energy of 4×10^{19} eV [8] from the Auger observatory. The upper limit for the photon fraction seems to increase to a significant fraction at the GZK cut-off, and one could naively pose that for higher energies, the allowed photon fraction is even larger. It should be noted that more observations of UHECRs could give a clearer, lower bound than already was determined. If a significant part of the annihilation product consists of photons, then the SHDM-annihilation scenario might be excluded.

A problem this top-down model faces is the lack of anisotropy, or rather an observed isotropic arrival distribution even for $> 10^{19}$ eV cosmic rays. This can be due to a large number of sources filling almost every region on the sky, or due to inter-galactic magnetic fields. Of course photons are not affected by magnetic fields, so they should point straight to their sources. Some degree of anisotropy can then be expected if ultra-high energy photons form a significant part of the flux, however there are clear constraints on the photon fraction.

Another loose end is the behaviour of SHDM in the early universe. We have shown that for our estimate of the cross section, the amount of dark matter annihilating in the dark halo Milky Way is small compared to the total amount of dark matter in the dark halo. However in the early universe the density of SHDM must have been much higher than at present. This would mean that in the early universe annihilation would have been abundant. Even though the annihilation rate scales with ρ^2, and thus an isotropic distribution of dark matter in the early universe would give the lowest possible annihilation rate, this early annihilation is still a problem that needs to be addressed.

There might still be a small window for SHDM as a source of UHECRs, but there are several problems to this scenario. If new data places tighter constraints on the photon flux, and if there remains a lack of anisotropy, this model might be excluded completely.

Bibliography

[1] K. Greisen. 'End to the cosmic-ray spectrum?!' In: *Phys. Rev. Lett* 16 (1966), p. 748.

[2] G.T. Zatsepin and V.A. Kuzmin. 'Upper limit of the spectrum of cosmic rays'. In: *JETP Lett.* 4 (1966), p. 78.

[3] Planck Collaboration et al. 'Planck 2015 results. XIII. Cosmological parameters'. In: *ArXiv e-prints* (2015). arXiv:1502.01589.

[4] Alessandro De Angelis and Mário João Pimenta. *Introduction to Particle and Astroparticle Physics*. ISBN: 978-88-470-2687-2. Springer Verlag, 2015.

[5] Pierre Auger Collaboration. 'Measurement of the cosmic ray spectrum above 4×10^{18} eV using inclined events detected with the Pierre Auger Observatory'. In: *jcap* 8, 049 (2015), p. 049. DOI: 10.1088/1475-7516/2015/08/049. arXiv: 1503.07786 [astro-ph.HE].

[6] http://www.physics.utah.edu/~whanlon/spectrum.html.

[7] Gijsbert Tijsseling. 'Modeling a dual mirror Cherenkov telescope to analyse pointing precision'. MA thesis. the Netherlands: Vrije Universiteit Amsterdam, 2014.

[8] Pierre Auger Collaboration et al. 'Upper limit on the cosmic-ray photon flux above 10^{19} eV using the surface detector of the Pierre Auger Observatory'. In: *Astroparticle Physics* 29 (2008), pp. 243–256. DOI: 10.1016/j.astropartphys.2008.01.003. arXiv: 0712.1147.

[9] In: ().

[10] John A. Peacock. *Cosmological Physics*. Ninth printing 2010. Cambridge, United Kingdom: Cambridge University Press, 1999.

[11] K. Garrett and G. Dūda. 'Dark Matter: A Primer'. In: *Advances in Astronomy* 2011, 968283 (2011). arXiv:1006.2483, p. 968283. DOI: 10.1155/2011/968283. arXiv: 1006.2483 [hep-ph].

[12] A. Schneider. 'Astrophysical constraints on resonantly produced sterile neutrino dark matter'. In: *jcap* 4, 059 (2016), p. 059. DOI: 10.1088/1475-7516/2016/04/059. arXiv: 1601.07553.

[13] M. Drewes. 'The Phenomenology of Right Handed Neutrinos'. In: *International Journal of Modern Physics E* 22, 1330019 (2013), p. 1330019. DOI: 10.1142/S0218301313300191. arXiv: 1303.6912 [hep-ph].

[14] E. Bulbul et al. 'Detection of an Unidentified Emission Line in the Stacked X-Ray Spectrum of Galaxy Clusters'. In: *apj* 789, 13 (2014), p. 13. DOI: 10.1088/0004-637X/789/1/13. arXiv: 1402.2301.

[15] A. Boyarsky et al. 'Unidentified Line in X-Ray Spectra of the Andromeda Galaxy and Perseus Galaxy Cluster'. In: *Physical Review Letters* 113.25, 251301 (2014), p. 251301. DOI: 10.1103/PhysRevLett.113.251301. arXiv: 1402.4119.

[16] P. W. Graham et al. 'Experimental Searches for the Axion and Axion-Like Particles'. In: *Annual Review of Nuclear and Particle Science* 65 (2015), pp. 485–514. DOI: 10.1146/annurev-nucl-102014-022120. arXiv: 1602.00039 [hep-ex].

[17] V. Berezinsky, M. Kachelrieß and M. Aa. Solberg. 'Supersymmetric superheavy dark matter'. In: *Phys.Rev.D78:123535* (2008). arXiv:0810.3012.

[18] Gary Felder, Lev Kofman and Andrei Linde. 'Instant Preheating'. In: *Phys.Rev.D59:123523* (1999). arXiv:hep-ph/9812289.

[19] Vadim A. Kuzmin and Igor I. Tkachev. 'Ultra High Energy Cosmic Rays and Inflation Relics'. In: *Phys.Rept.320:199-221* (1999). arXiv:hep-ph/9903542.

[20] Edward W. Kolb, Alessio Notari and Antonio Riotto. 'On the reheating stage after inflation'. In: *Phys.Rev.D68:123505* (2003). arXiv:hep-ph/0307241.

[21] Edward W. Kolb, Daniel J.H. Chung and Antonio Riotto. 'WIMPZILLAS!' In: *FNAL-CONF-98/325A* (1998). arXiv:hep-ph/9810361v1.

[22] A.H. Campos, J.M.F. Maia and R. Rosenfeld. 'Instant preheating mechanism and UHECR'. In: *Phys.Rev.D70:023003* (2004). arXiv:astro-ph/0402413.

[23] Lev Kofman, Andrei Linde and Alexei A. Starobinsky. 'Towards the Theory of Reheating After Inflation'. In: *Phys.Rev.D56:3258-3295* (1997). arXiv:hep-ph/9704452.

[24] A.H. Campos et al. 'Bounds on Direct Couplings of Superheavy Metastable Particles to the Inflaton Field from Ultra High Energy Cosmic Ray Events'. In: *Mod.Phys.Lett. A17 2179-2188* (2002). arXiv:hep-ph/0108129.

[25] P. Bhattacharjee and G. Sigl. 'Origin and propagation of extremely high energy cosmic rays'. In: *physrep* 327 (2000), pp. 109–247. DOI: 10.1016/S0370-1573(99)00101-5. eprint: astro-ph/9811011.

[26] Jürg Diemand and Ben Moore. 'The structure and evolution of cold dark matter halos'. In: *Advanced Science Letters, 4, 2, 297* (2011). arXiv:0906.4340v1.

[27] J. Diemand et al. 'Clumps and streams in the local dark matter distribution'. In: *Nature 454:735-738* (2008). arXiv:0805.1244v2.

[28] Marcel Zemp. 'The Structure of Cold Dark Matter Halos: Recent Insights from High Resolution Simulations'. In: *Mod.Phys.Lett.A24:2291-2305* (2009). arXiv:0909.4298v1.

[29] J.R. Primack et al. 'Formation of Dark Matter Halos'. In: *Galaxy Dynamics, proceedings of a conference held at Rutgers University, 8-12 Aug 1998. ASP Conference Series vol. 182* (1999). arXiv:astro-ph/9812241v1.

[30] J. Stadel et al. 'Quantifying the heart of darkness with GHALO - a multi-billion particle simulation of our galactic halo'. In: *MNRAS (2009) 398 (1): L21-L25* (2009). arXiv:0808.2981v2.

[31] http://www.ucolick.org/~diemand/vl/images.html.

[32] M. Einasto et al. 'The richest superclusters. I. Morphology'. In: *aap* 476 (2007), pp. 697–711. DOI: 10.1051/0004-6361:20078037. arXiv: 0706.1122.

[33] P. Blasi and A. V. Olinto. 'Magnetized local supercluster and the origin of the highest energy cosmic rays'. In: *prd* 59.2, 023001 (1999), p. 023001. DOI: 10.1103/PhysRevD.59.023001. eprint: astro-ph/9806264.

[34] E. Roulet and for the Pierre Auger Collaboration. 'Recent results from the Pierre Auger Observatory'. In: *ArXiv e-prints* (2015). arXiv: 1503.09173 [astro-ph.HE].

[35] F. Nesti and P. Salucci. 'The Dark Matter halo of the Milky Way, AD 2013'. In: *jcap* 7, 016 (2013), p. 016. DOI: 10.1088/1475-7516/2013/07/016. arXiv: 1304.5127.

[36] P. Lipari. 'The lifetime of cosmic rays in the Milky Way'. In: *ArXiv e-prints* (2014). arXiv: 1407.5223 [astro-ph.HE].

Appendices

Appendix A: Particle creation

Here we will show that we only need to take the first swing of ϕ into account. First we use equation 5.9 in its general form

$$n_\chi = \frac{(g|\dot{\phi}_0|)^{3/2}}{(2\pi)^3}\exp\left(-\frac{\pi m_\chi^2}{g|\dot{\phi}_0|}\right). \tag{8.1}$$

If we take equation 4.7 again

$$\phi(t) \approx \frac{M_p}{3}\frac{\sin(mt)}{mt}, \tag{8.2}$$

we can take the derivative

$$\dot{\phi}(t) \approx \frac{M_p}{3}\frac{\cos(mt)}{t} - \frac{M_p}{3}\frac{\sin(mt)}{mt^2}. \tag{8.3}$$

It might be more intuitive now to write the equation in terms of the number of swings of ϕ. We can define the number of oscillations as $2\pi N = mt$, such that whenever $N = 1/2, 1, 3/2, ...$ ϕ has a minimum. We then get

$$\dot{\phi}(t) \approx \frac{M_p}{3}\frac{m\cos(2\pi N)}{2\pi N} - \frac{M_p}{3}\frac{m\sin(2\pi N)}{(2\pi N)^2}. \tag{8.4}$$

At the first crossing $N = 1/2$ and

$$|\dot{\phi}_0^{(1)}| = \frac{M_p}{3}\frac{m}{\pi}. \tag{8.5}$$

At the second crossing for $N = 1$ this is

$$|\dot{\phi}_0^{(2)}| = \frac{M_p}{6}\frac{m}{\pi} = \frac{1}{2}|\dot{\phi}_0^{(1)}|. \tag{8.6}$$

We then take the ratio between n_χ for $\dot{\phi}_0^{(2)}$ and $\dot{\phi}_0^{(1)}$, we obtain

$$\frac{n_\chi^{(2)}}{n_\chi^{(1)}} = \left(\frac{|\dot{\phi}_0^{(2)}|}{|\dot{\phi}_0^{(1)}|}\right)^{3/2}\exp\left(-\frac{\pi m_\chi^2}{g|\dot{\phi}_0^{(2)}|} + \frac{\pi m_\chi^2}{g|\dot{\phi}_0^{(1)}|}\right) \tag{8.7}$$

$$= \left(\frac{1}{2}\right)^{3/2}\exp\left(-\frac{\pi m_\chi^2}{g|\dot{\phi}_0^{(1)}|}\right) \tag{8.8}$$

$$= \left(\frac{1}{2}\right)^{3/2}\exp\left(-\frac{3\pi^2 m_\chi^2}{gmM_p}\right). \tag{8.9}$$

Filling in the same values for the variables as in section 5.1, namely $g = 10^{-4}$, and $m_\chi \sim 10^{14}\text{GeV} = 10^{-5} M_p$ we see that

$$\frac{n_\chi^{(2)}}{n_\chi^{(1)}} \sim 10^{-13}\,. \tag{8.10}$$

This means that practically all particles are created in the first swing, and we can ignore subsequent crossings of the inflaton field after the first crossing.

Appendix B: Fraction of annihilating dark matter

Based on the rate of dark matter annihilation from equation (7.16), we will determine the amount of dark matter that annihilates relative to the total amount of dark matter in the dark halo of the Milky Way. We integrate the Burkert density profile given in equation (6.4) to a radius of 100 kpc,

$$M_{\text{DM}} = \int_0^{100} 4\pi\, r^2 \frac{\rho_0}{(1 + r/R)(1 + (r/R)^2)} dr\,. \tag{8.11}$$

We use a central density $\rho_0 = 4 \times 10^7\ \text{M}_\odot\ \text{kpc}^{-3}$ and a scale radius of $R = 9.26$ kpc [35]. The integral gives a mass of

$$M_{\text{DM}} = 7 \times 10^{11}\ \text{M}_\odot\,. \tag{8.12}$$

The number of DM particles is thus this mass divided by a ψ mass of $\sim 10^{14}$ GeV,

$$n_{\text{DM}} \approx 8 \times 10^{54}\,. \tag{8.13}$$

Taking an annihilation rate of $7.76 \times 10^{30}\text{s}^{-1}$ from equation (7.16), it would mean that each second a part

$$\frac{2 * 7.76 \times 10^{30}}{8 \times 10^{54}}\text{s}^{-1} \approx 2 \times 10^{-24}\text{s}^{-1} \tag{8.14}$$

of the current dark matter particles in the 100 kpc sphere annihilate. If this annihilation rate is constant, then over a time of 10 Gyr a fraction of

$$2 \times 10^{-24}\text{s}^{-1} \times 10\text{Gyr} \approx 6 \times 10^{-7} \tag{8.15}$$

of the amount of particles in the current halo has annihilated. This is a small fraction, which ensures our halo does not completely annihilate on these timescales.